YILDIZ TECHNICAL UNIVERSITY
DEPARTMENT OF MECHANICAL ENGINEERING

THE VISCOELASTIC MATERIAL CHARACTERIZATION AND GRAPHENE-EPOXY NANOCOMPOSITE APPLICATIONS IN THE ANSYS

16065175 MERT ÖZKAYAHAN

PREPARED AT CONSTRUCTION DIVISION

GRADUATION THESIS

Advisor: PROF. DR. ÖZGEN ÜMİT ÇOLAK ÇAKIR

İSTANBUL, 2021

TABLE OF CONTENTS

Page

SYMBOL LIST

E	Young's modulus [P]
t	Time [s]
G	Relaxation modulus [P]
n	Number of Prony terms
L	Length [m]
u	Nodal displacement [m]
M	Mach number
Re	Reynolds number
P	Pressure [P]
T	Temperature [K]
V	Velocity [m/s]

Greek Letters

σ	Stress [P]
τ	Relaxation time
α	Relative moduli
ρ	Density [kg/m^3]

Index

t	Total
s	Spring
d	Damper

ABBREVIATION LIST

CFD	Computational Fluid Mechanics
FSI	Fluid Structural Interaction
CPU	Central Processing Unit

FIGURE LIST

ABSTRACT

The behavior of the viscoelastic material of the polymer was investigated. The Maxwell model, the Voigt model, and the Prony Series approach were introduced as model types that characterize viscoelastic behavior. The finite element method which is the background of numerical analysis programs such as ANSYS was explained. Araldite LY 564 epoxy and graphene-epoxy nanocomposite fabrication studies conducted at Yıldız Technical University Central Laboratory by Özgen Çolak Çakır were followed and reported. To characterize Araldite LY 564 epoxy material, some tests were performed in laboratory conditions. In this thesis, these materials were introduced to the ANSYS program and the simulations of the quasi-static, relaxation tests were done in the ANSYS Static Structural module. To simulate the relaxation test, the Prony Series approximation was adopted. NACA 0012 airplane wing FSI analysis, electronic card drop test and car body crash analysis were performed in the ANSYS with graphene-epoxy and other materials which are popular and prevalently used for these sectors. The results were compared and interpreted.

Keywords: Viscoelasticity, Graphene-Epoxy Nanocomposite Materials, Finite Element Method

1. INTRODUCTION

Wood, rubber, cotton, wool, leather, and silk are examples of naturally occurring polymers generated from plants and animals that have been used for ages. The determination of the molecular structures of this category of materials, as well as the production of countless polymers built from tiny organic molecules, has been made feasible by modern scientific research instruments. Synthetic polymers make up a large portion of the plastics, rubbers, and fiber materials we use. Indeed, the introduction of synthetic polymers has essentially transformed the science of materials since the end of World War II. Synthetics can be made cheaply, and their qualities can be modified to the point that many of them outperform their natural equivalents. Metal and wood pieces have been replaced in some applications by plastics, which have sufficient characteristics and can be produced at a cheaper cost [1].

When compared to other structural materials such as metals, the magnitudes of time and temperature dependency of mechanical characteristics of polymers are of critical relevance. Understanding viscoelastic behavior is therefore essential for effective polymer application. Most of the polymers are classified as viscoelastic bodies. These materials react to external pressures in a way that is halfway between that of an elastic solid and that of a viscous liquid, as the name indicates [2].

When one considers the intricate molecular adjustments that must be underlying any macroscopic mechanical deformation, the dominance of viscoelasticity in polymers is unsurprising. Atoms are displaced from equilibrium positions in fields of force that are extremely local in nature during the deformation of hard solids such as diamond, sodium chloride, or crystalline zinc; elastic constants may be determined using knowledge of the interatomic potentials. Other mechanical phenomena are caused by structural flaws involving distances that are not atomically great. Viscous flow in an ordinary liquid composed of small molecules reflects the change in the distribution of molecules surrounding a given molecule over time and under stress; here, too, the relevant forces and processes of readjustment are quite local in nature, and the viscosity can be calculated in principle from a knowledge of them. Each flexible threadlike molecule in a polymer, on the other hand, has an average volume far larger than atomic dimensions and is constantly altering the form of its contour as it wriggles and writhes with its thermal energy. Under stress, a new set of configurations emerges; the reaction to the local features of the new distribution is fast, the reaction to the long-range aspects

is gradual, and the reaction of such a system to the external system spans a large and continuous-time scale [3].

The equation (1.1) is the equation form of the left graph and formulize that the elastic behavior of the materials. The equation (1.2) is the equation form of the right graph and formulize that the viscoelastic behavior of the materials.

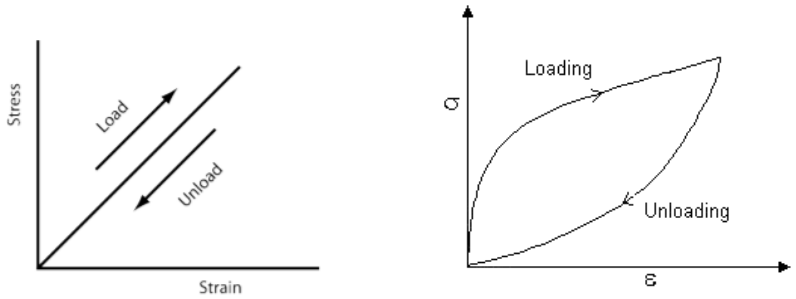

Figure 1.1 Elastic behavior of materials(left) and viscoelastic behavior of materials(right)

$$\sigma = E.\varepsilon \quad (1.1)$$

$$\sigma = \mu \frac{d\varepsilon}{dt} \quad (1.2)$$

Graphene

Since Andre Geim and Kostya Novoselov first discovered single-layer graphene in 2004, this atomically thin carbon sheet has gotten a lot of interest and has become a quickly rising star on the horizon of materials research. For example, the European Commission recently funded the European Graphene Flagship, a 10-year research effort that includes more than 140 academic and industrial organizations from 23 countries and gives 1 billion euros in financing.

Because of its superior performance in mechanical, electrical, and thermal applications, graphene has lately aroused academic and industrial attention. When properly included, graphene can considerably improve the physical characteristics of epoxy at extremely low loadings [4].

2. LITERATURE RESEARCH

In the study of Colak et al [5], the mechanical characterization of Araldite LY 564 Epoxy is investigated by performing creep, relaxation, quasi-static compression, and high strain rate behavior tests. In the other study of Colak et al [6], the high strain rate behavior of graphene-epoxy nanocomposite is investigated. In the work by Fettahoglu [7], the modeling for relaxation of a viscoelastic material for different temperature values by using the Prony series is investigated. In the article by Zheng et al. [8], the viscoelastic material model to simulate relaxation in glass transition study is done in the ANSYS finite element program. In the study of Ganesh et al. [9], the CFD analysis of the NACA 0012 airplane wing is done in ANSYS. Liang et al. [10], investigated the fabrication of graphene-based electronic circuits and memory cards. The environmental and human health impacts of the graphene-based nanomaterials are investigated by Fadeel et al [11].

2.1 Viscoelastic material models

The material could be anything that is uniform and isotropic, be it a polymer, metal, biological tissue, or clay. As our focus is polymers, it is desirable to consider the representation of linear viscoelastic processes by certain model systems to gain greater insight into relaxation behavior and eventually its relationship to structure. In this section, three viscoelastic material models will be introduced briefly.

2.1.1 The Maxwell model

The Maxwell model, which consists of a spring and a dashpot in series as can be seen in the Figure 2.1, is the simplest approach to simulate viscoelasticity. This model is helpful because it is simple to understand and depicts several important features of viscoelastic materials, such as creep. However, because there is no limit on how far the dashpot may expand, this model is not suited for representing materials over lengthy periods of time [12].

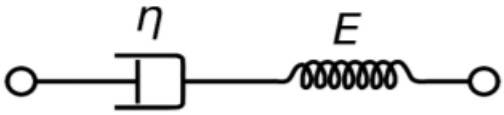

Figure 2.1 The Maxwell model [12]

As components are in series, force is equal in each:

$$\sigma_t = \sigma_s = \sigma_d \quad (2.1)$$

Total extension is sum of the extension of each component:

$$\varepsilon_t = \varepsilon_s + \varepsilon_d \quad (2.2)$$

Differentiating the equations (4) gives

$$\frac{d\varepsilon_t}{dt} = \frac{d\varepsilon_s}{dt} + \frac{d\varepsilon_d}{dt} \quad (2.3)$$

Differentiating the equations (1) with respect to time and rearranging gives

$$\frac{d\varepsilon_s}{dt} = \frac{1}{E} \cdot \frac{d\sigma_s}{dt} \quad (2.4)$$

Rearranging equation (2) gives:

$$\frac{d\varepsilon_d}{dt} = \frac{\sigma_d}{\mu} \quad (2.5)$$

Substituting equations (6) and (7) into (5)

$$\frac{d\varepsilon_t}{dt} = \frac{1}{E} \cdot \frac{d\sigma_s}{dt} + \frac{\sigma_d}{\mu} \quad (2.6)$$

Integrating (8) with respect to t gives

$$\varepsilon_t = \frac{\sigma_s}{E} + \frac{\sigma_d}{\mu} t \quad (2.7)$$

The Maxwell model predicts that when a stress is applied, there will be an immediate extension from the spring followed by an undefined extension from the dashpot as a function of time, as indicated by the preceding equations.

2.1.2 The Voigt model

The Voigt model has the same basic components as the Maxwell model, with the exception that the spring and dashpot are in parallel rather than series. The Voigt model describes a viscoelastic solid in the simplest feasible form because of this arrangement. The model's restriction is that the strain in both components must be the same. The total stress must then equal the sum of the stresses in the two separate parts [2].

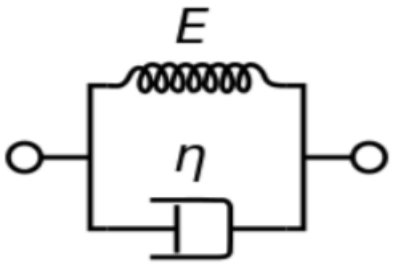

Figure 2.2 The Voigt model [12]

In the Voigt configuration, the two elements are connected in parallel and both elements are subjected to the same strain but different stress:

$$\sigma_t = \sigma_s + \sigma_d \quad (2.8)$$

$$\varepsilon_s = \varepsilon_d \quad (2.9)$$

Because of equal strain in both elements, the model is also known as an *iso-strain model.* The basic equation for the stress in the Kelvin-Voigt model is:

$$\sigma = E.\ \varepsilon + \mu\frac{d\varepsilon}{dt} \quad (2.10)$$

2.1.3 The Prony Series method

The deformation history must be addressed while determining the time-dependent stress-strain state in a linear viscoelastic material under an arbitrary loading process.

These historical impacts are included in the time-dependent constitutive equations of a solid viscoelastic material. To derive the constants in the constitutive equations, the load (stress) and displacement (strain) history, the loading rate (displacement rate), and the time of load application on the specimen are all required. A Prony series is a frequent form for these constitutive equations [13]:

$$G(t) = G_0 \left[\alpha_\infty^G + \sum_{i=1}^{n_G} \alpha_i^G \exp\left(-\frac{t}{\tau_i^G}\right)\right] \quad (2.11)$$

G_0 =Relaxation moduli at t=0

n_G = Number of Prony terms

α_i^G = Relative moduli

τ_i^G = Relaxation time

2.2 Finite element method

The human mind's limitations are such that it is unable to comprehend the behavior of its complex surroundings and creations in a single action. Thus, the engineer, scientist, or even economist proceeds by dividing all systems into their individual components or elements, whose behavior is easily known, and then reconstructing the original system from such components to investigate its behavior.

In many cases, an appropriate model may be created by combining a small number of well-defined components. We term such systems discrete. In others, the subdivision is continued indefinitely, and the problem can only be defined by using the mathematical fiction of an infinitesimal. As a result, differential equations, or similar statements with an unlimited number of components emerge. Such systems are referred to as continuous systems.

Discrete problems, even those with a huge number of elements, may now be handled quickly thanks to advances in computer technology. Continuous issues can only be addressed precisely by mathematical manipulation due to the finite capacity of all

computers. The available mathematical techniques for exact solutions usually limit the possibilities to overcome simplified situations [14].

Stress, thermal, dynamics, vibration, buckling, deformation, optimization, and topology analyses can be done by applying finite element method. Thanks to this method, failures and insufficiencies in the system can be detect during design process. Finite element method is used various sectors such as space-aviation, automotive, biomedical, production, buildings like bridges. There are some requirements while applying this method; remembering that this method is an approximation, the system that will be analyses must be planned appropriately, detecting boundary conditions correctly, the analysist must have enough ability and experience to provide reliable results.

For static cases, the system of equilibrium can be stated as:

$$[K]\{D\} = \{F\} \tag{2.12}$$

The displacement vector {D} contains displacements of 3n degrees of freedom, where n is the number of nodes. The force vector of {F} contains forces acting on all degrees of freedom. The matrix [K] is called the stiffness matrix of the structure.

The first step of the applying finite element method for solving a problem is identifying bodies' geometries, material properties, support conditions, and loading conditions. The body is divided into as possible as small components. Then, the equation (2.12) is established by constructing the [K] matrix according to the elements' geometries and the material properties. Most of the components in {F} can be calculated according to the loading conditions. Although, most of the components in {D} are unknown, some components, however, are known according to the support conditions. The total numbers of unknowns in {D} and {F} should be equal to the total number of degrees of freedom of the structure. When the equation (2.13) is solved, the nodal displacements{d} of each element are known.

$$\{u\} = [N]\{d\} \tag{2.13}$$

For each element, displacement field {u} is calculated by using an interpolation method. The interpolation functions in [N] are called the shape functions. As the last step, according to the strain-displacement relations, strain field is calculated, and according to the stress-strain relations, stress field is calculated.

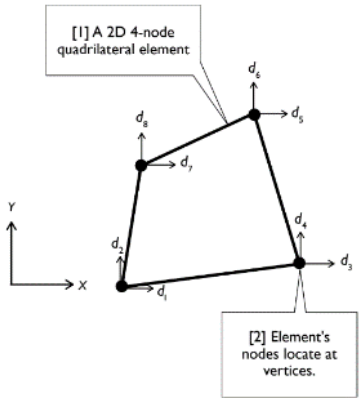

Figure 2.3 The example of the element in the finite element method.

In the dynamic analyses, deformations and boundary conditions are depended on time. If the system that will be analysed has small loading velocity, it can be conducted in the Static Structural module as non-linear analyses, but for such models like explosion, crash, drop conditions are performed in the Explicit Dynamic module due to high loading velocity according to the time. In the analysis programs, dynamic analyses are solved according to general equation of motion (2.14).

$$[M]\{u''\}+[C]\{u'\}+[K(u)]\{u\}D=\{F(t)\} \quad (2.14)$$

[M]: structural mass matrix

[C]: structural damping matrix

[K]: structural stiffness matrix

{F}: the load vector

{u''}: nodal acceleration vector

{u'}: nodal velocity vector

{u}: nodal displacement vector

(t): time

The explicit dynamics uses the principle of energy conservation to monitor the solution accuracy as explained in equation (2.15):

(Reference Energy) + (Work Done) = (Current Energy) (2.15)

The overall energy is calculated for each cycle by the program and is compared with the

energy differences in each cycle. This called as energy error method and if it passes the 10% threshold value, solution is regarded as unstable and stops.

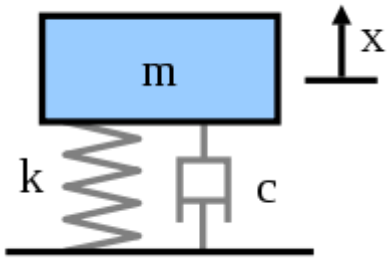

Figure 2.4 The model of the general equation of motion.

3. EXPERIMENTAL WORKS

3.1 Material preparation

In this section, the producing processes of Araldite LY 564 Epoxy and Graphene-Epoxy with the graphene content of 0.1% nanocomposite material will be introduced briefly. These materials were produced in Yıldız Technical University Central Laboratory in the study of TUBITAK research project which is conducted by Özgen Çolak.

3.1.1 The preparation of Araldite LY 564 Epoxy

The desired amount of hardener and epoxy weights were measured and mixed. Secondly, the mixing is stirred with a magnetic stirrer for nearly half an hour. At the end of this process, the gas removing process was done by a vacuum chamber to remove porosities. After that, the mixture was poured into silicon molds and cured for nearly 5 hours at different specified temperatures.

3.1.2 The preparation of Graphene-Epoxy nanocomposite

The weight of the graphene flakes produced by the electric arc discharge method was measured with a precision scale then, mixed with pure water and triton at specified rates to functionalize the material. The mixture was placed in a sonication homogenizer to obtain smaller graphene particles. After this operation, the mixture was stirred with a magnetic stirrer for almost half of a day. To obtain a more purified solution, the mixture was filtered for a couple of hours and was placed in a vacuum chamber for removing excessive gases to reduce porosities. Epoxy was added to the mixture and stirred again with a magnetic stirrer. After this operation, the mixture was got more homogenized by a three-roll milling machine. Then, the hardener was added to the mixture and stirred again with a magnetic stirrer. To remove the porosities the mixture was placed into the vacuum chamber again, after a specified time the bubbles that remained in the mixture

were removed by a device called a torch, and the mixture was replaced in a vacuum chamber once more. As a last step of the fabrication, the prepared mixture was poured into molds and cured for nearly 5 hours at different specified temperatures.

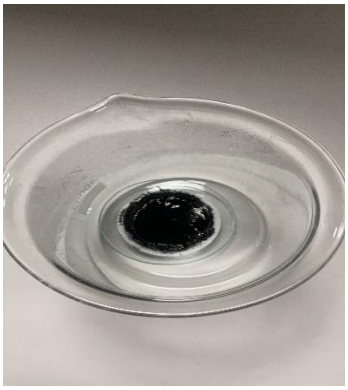

Figure 3.1 Functionalized graphene flakes(left), graphene-epoxy nanocomposite specimens(right)

3.2 Material testing and simulating in the ANSYS

To characterize the Araldite LY 564 Epoxy produced; compression, relaxation, creep tests were performed in laboratory conditions and results are released in the work by Colak et al. [5]. Considering the test results, the behaviour of Araldite LY 564 Epoxy was tried to introduce to ANSYS. By using test data conducted in the laboratory, basic models are set up in the program, and obtaining relatively realistic results were aimed. In this section, some brief information will be given about these tests and analysis simulated in the ANSYS finite element method program.

3.2.1 Compression Testing

When examining some of a material's basic mechanical characteristics, the simple compression technique of testing offers numerous inherent advantages. The compression test is used to determine elastic limit, proportional limit, yield point, yield strength, and (for some materials) compressive strength. It is easy to use, uses a tiny

amount of material, has a basic sample shape, does not require expensive grips (like those used in tensile testing), and is resistant to instabilities like necking. As a result, it is increasingly being utilized to assess the mechanical characteristics of a variety of materials. It is particularly useful for determining the modulus and strength of a wide range of composites, as well as analyzing the strain-hardening behavior of a variety of metals and polymers [15].

The quasi-static compression test was done in the study Colak et al, using Instron 5982 (100 kN capacity) universal static test device. Tests are conducted on the cylindrical-shaped specimens with a diameter of 11 mm and a length of 10 mm at room temperature for different strain rates. The testing machine is constituted by a load cell, a compression plate, a loading frame, and a table that hold the specimen. While quasi-static compression testing, the compression plate goes down and compress the specimen by 0,01 stain rate until fracture occurs. The strain gauges measure the strain level of the specimen, and the data is transferred the computer.

Figure 3.2 Instron 5982 (100 kN capacity) universal static test device.

3.2.1.1 Quasi-static compression test simulation in the ANSYS

In this analysis, Araldite LY 564 Epoxy material's stress-strain graph is tried to be obtained by using data from results of quasi-static compression test which was conducted in the laboratory. In the work by Colak et al. [5], the behaviour of Araldite LY 564 Epoxy under quasi-static compression was investigated at strain rates of 0,001, 0,01, 0,1. The properties of Araldite LY 564 Epoxy were taken from this study by

considering 0,01 strain rate quasi-static conditions.

Firstly, to conduct this analysis in ANSYS, it must be determined which module will be used. Velocity is one of the crucial parameters for decision, static structural module is offered for static or low-speed conditions. Generally, if a system has under 0.1 mm/s velocities, it means that a static structural module is proper for such analysis. Since my simulation is a quasi-static compression test that has a 0.01 strain rate, I conducted my analysis by using static structural.

The second step is defining a new material into ANSYS via engineering data. Since, Araldite LY 564 Epoxy shows nonlinear behaviour in the tests, properties of elasticity and plasticity must be introduced to the program. As elastic properties, the values of Young's modulus and Poisson's ratio were introduced to the program. As for plasticity, multilinear isotropic hardening is added by introducing the plastic strain and stress data set which are obtained by laboratory experiment.

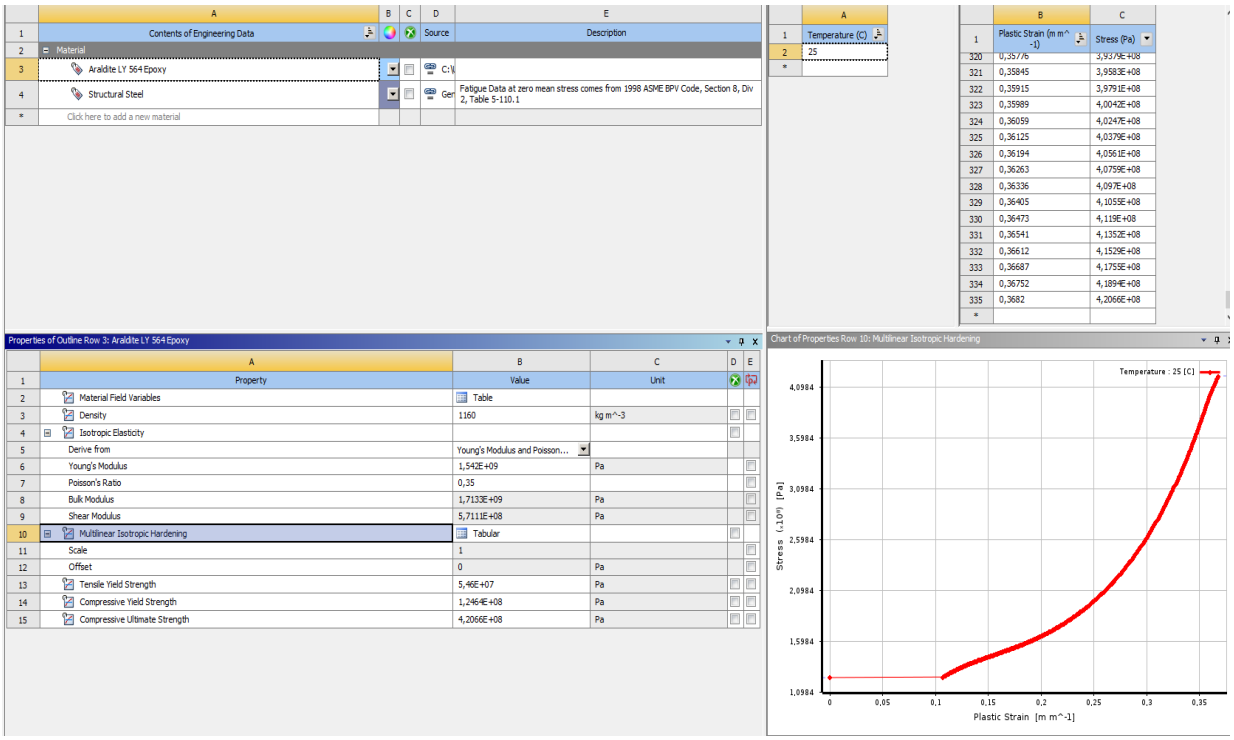

Figure 3.3 Engineering data section in the ANSYS.

After defining the material, the geometry of the part which will be analysed was imported to the ANSYS. The part is a cylindrical-shaped specimen with a diameter of 11 mm and a length of 10 mm at room temperature. As the last step, the mesh structure and analysis settings were created in the model section. To provide a good quality mesh structure, the multizone mesh method was used with hexa/prism mesh type. For the up

and bottom side of the specimen, the face meshing method was used to obtain better results. In the last stage of meshing, the mesh element size for the whole body was decreased to 3 mm. To model the simulation, the bottom side of the specimen identified as fixed support, and tabular displacement was given on the other side of the specimen. When it comes to the analysis settings, according to the article, the strain rate is 0.01 1/s and the total strain value is 0.38 mm. So, it means that our analysis should include 38 steps. Considering this, the displacement value for each step obtained by using the with equation (3.1). Each displacement value was introduced to the program by starting at 0.1 mm for the first second and by reaching a 3.5 mm total displacement value.

$$\varepsilon = \frac{L_0 - L}{L_0} \qquad (3.1)$$

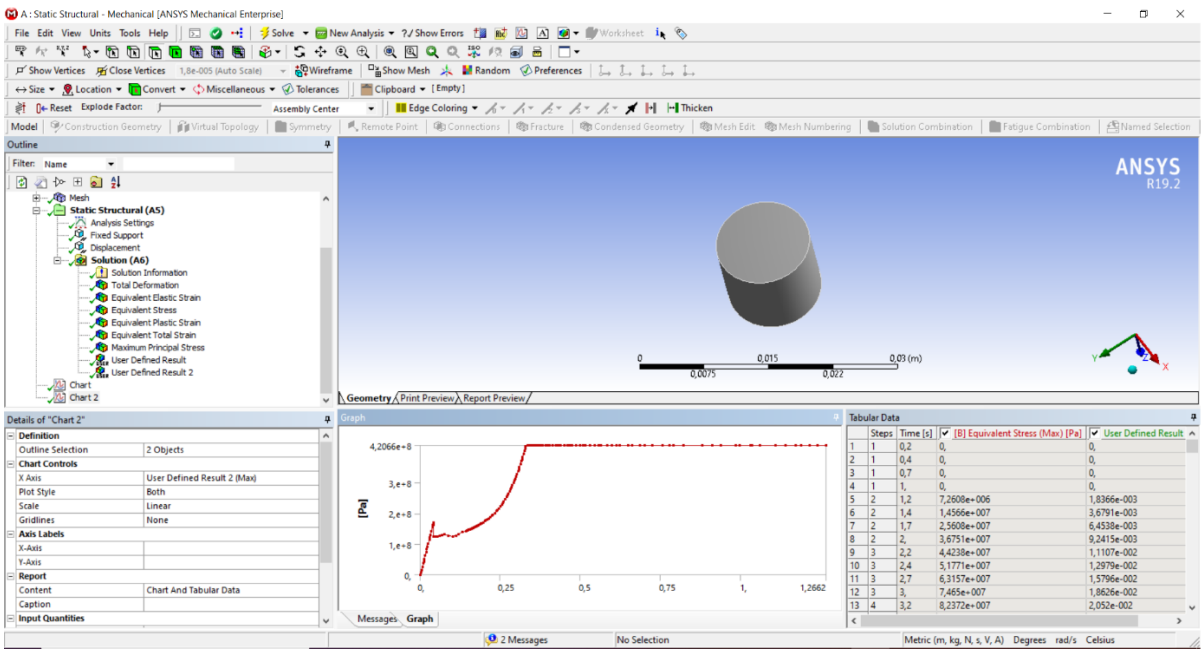

Figure 3.4 The compression test results of Araldite LY 564 Epoxy in the ANSYS.

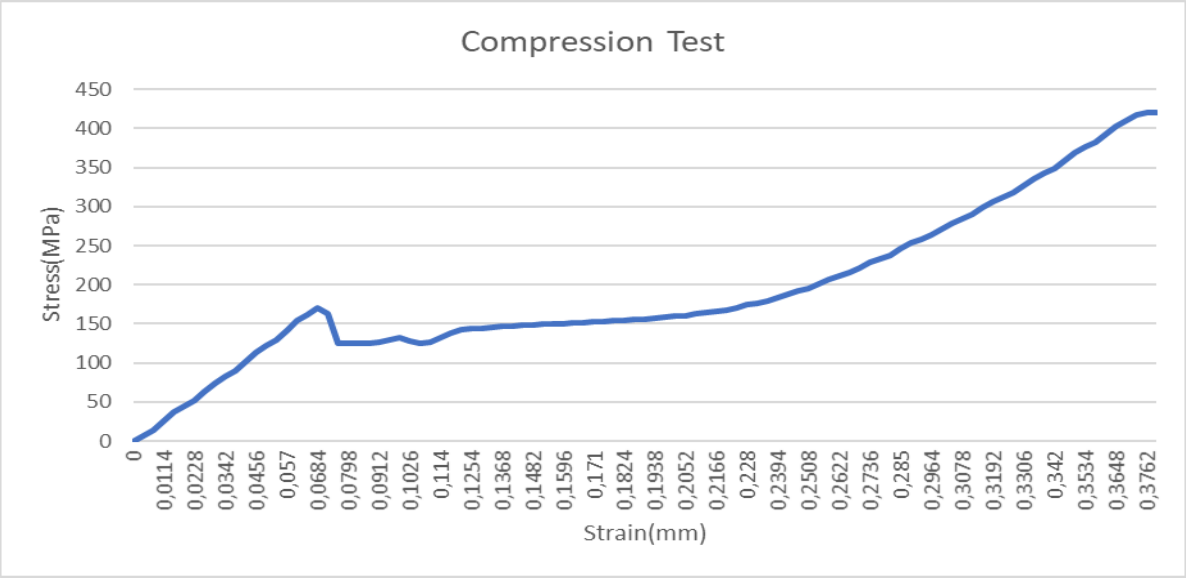

Figure 3.5 Stress-strain graph of the compression test according to the ANSYS results.

As can be seen in Fig. 1, the stress-strain graph for quasi-static compression test is obtained in ANSYS. In general perspective, this graph is found to be compatible with the other graphs in literature. When comparing with the laboratory test results, this graph largely corresponds to real test results. Until reaching 0,07 strain value, viscoelastic material presented the elastic behavior and necking occurred at just above 150 MPa. After this point, the effect of viscoelasticity is observed, and the stress value occurred its peak at roughly 410 MPa which is fracture point.

3.2.2 Relaxation testing

Under constant strain, stress relaxation is a steady decrease in stress. This is especially important in applications where the component is subjected to continuous forces during application and the parts' qualities must be maintained throughout the process. Applications such as carbonated beverage bottle caps, snap-fit assemblies, sealants, electrical contacts, and gaskets must all be developed with the stress relaxation behavior of the material in consideration. The stress-relaxation phenomena is used by numerous researchers to analyze the viscoelastic nature of plastics. In analytic software, creep models are frequently used to anticipate stress relaxation.

The decreased tendency of plastic materials to return to their original position after being loaded might alternatively be defined as stress relaxation. The samples are distorted to a preset level of strain to test this attribute. The amount of load needed to keep the strain constant is then calculated over time. A specimen is stretched to a given length in an experimental setting, and the resulting stress is measured. The specimen is stretched in that posture for an extended length of time. Stress decay occurs when the amount of load necessary to maintain a strain decreases over time. Stress relaxation results in stress decay [16].

A material's relaxation is often measured during creep testing on a universal testing machine (Figure3.2). When measuring relaxation, the motion of the crosshead is stopped, and the load cell continues to monitor forces to calculate the reduction in stress of the material.

The specimen is swiftly distorted a certain amount in stress relaxation experiments, and the stress required to maintain the deformation is recorded as a function of time. For a theoretical knowledge of viscoelastic materials, stress relaxation studies are critical. In the relaxation test, the stress in a viscoelastic material will gradually diminish over time [17]. The mathematical representation of the stress relaxation curve is:

$$\sigma(t) = \sigma_0 . e^{-t/\tau} \quad (3.2)$$

where σ_0 is the initial stress. The viscoelastic function obtained is the stress relaxation modulus, E(t), that is defined as:

$$G(t) = \frac{\sigma(t)}{\varepsilon_0} \quad (3.3)$$

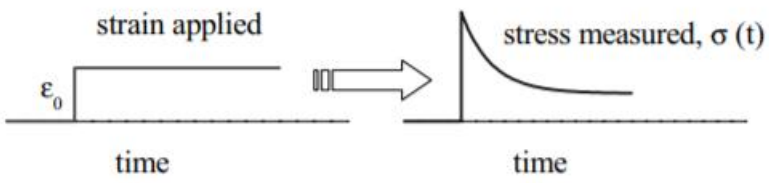

Figure 3.6 The strain-time graph(left) and the stress-time graph(right) for the relaxation test.

3.2.2.1 Relaxation test simulation in the ANSYS

Generalized Maxwell elements and the Prony series are two approaches used by ANSYS to simulate the viscoelastic material behavior of bodies. Because the Prony series approach is more robust and dependable than the generalized Maxwell elements technique, it was employed to depict stress relaxation in this work.

As the first step of modelling, isotropic elasticity and density values are written in the program. To define the viscoelastic property, Shear Data-Viscoelastic and Prony Shear Relaxation properties were added to the material property section. When Shear Data-Viscoelastic is added to the property section, the shear modulus and time data are asked by the program. Modulus values are calculated with equation 16 and uploaded to the ANSYS. After uploading the viscoelastic shear data to the ANSYS, Prony series constants were calculated by the program by curve fitting. For curve fitting, temperature values and seed values are defined. Seed values are important parameters in terms of defining time-dependent behaviour, were chosen proportionally starting from 1 and reaching 7200 which is the total time of the experiment. 6 terms of Prony series constants were calculated to the ANSYS. Curve fitting is a crucial factor for defining material to the program properly and must be checked before continuing with the other steps.

The geometry of the part to be studied was imported into ANSYS Static Structural module once the material was defined. At room temperature, the portion is a cylindrical-shaped specimen with a diameter of 11 mm and a length of 10 mm. In the model section, the mesh structure and analysis parameters were generated as the last stage. The multizone mesh approach was utilized with the hexa/prism mesh type to generate a high-quality mesh structure. Face meshing was utilized to improve the findings on the specimen's top and bottom sides. The mesh element size for the overall body was reduced to 5 mm in the final step of meshing.

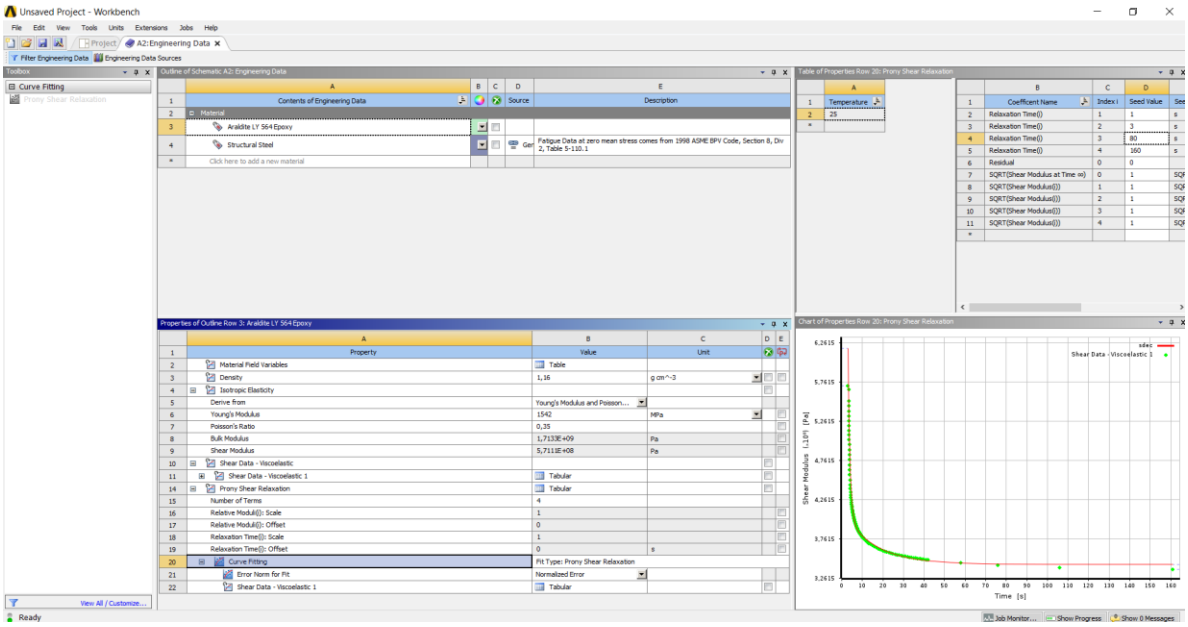

Figure 3.7 The material configuration of Araldite LY 564 Epoxy.

Since the experiment in laboratory condition takes 7200 seconds which is too long for simulating in the ANSYS, the total time-period must be minimized while defining time-step depending on computer CPU. To minimize the total time, the first 161 seconds of test data was used for the simulation.

The time determinations for compression and relaxation periods are done by selecting plausibly time values. While the bottom side of the specimen identified as fixed support, displacement applied to the upper side of the specimen. 2 time steps are identified in analysis settings to simulate the relaxation test. The first step is 3,5 seconds for the compression and the second step is 157,5 seconds for the relaxation. The large deflection option must be turned to be on to add to non-linear effects that are crucial for such viscoelastic problems in the ANSYS.

The displacement was defined as ramped with 3,5 mm for the 3,5 seconds to model compression process and for the remaining 157,5 seconds displacement was arranged as remaining stable to model the relaxation process. As the last step of modeling, the thermal condition inserted into the specimen was 25 ℃temperature value.

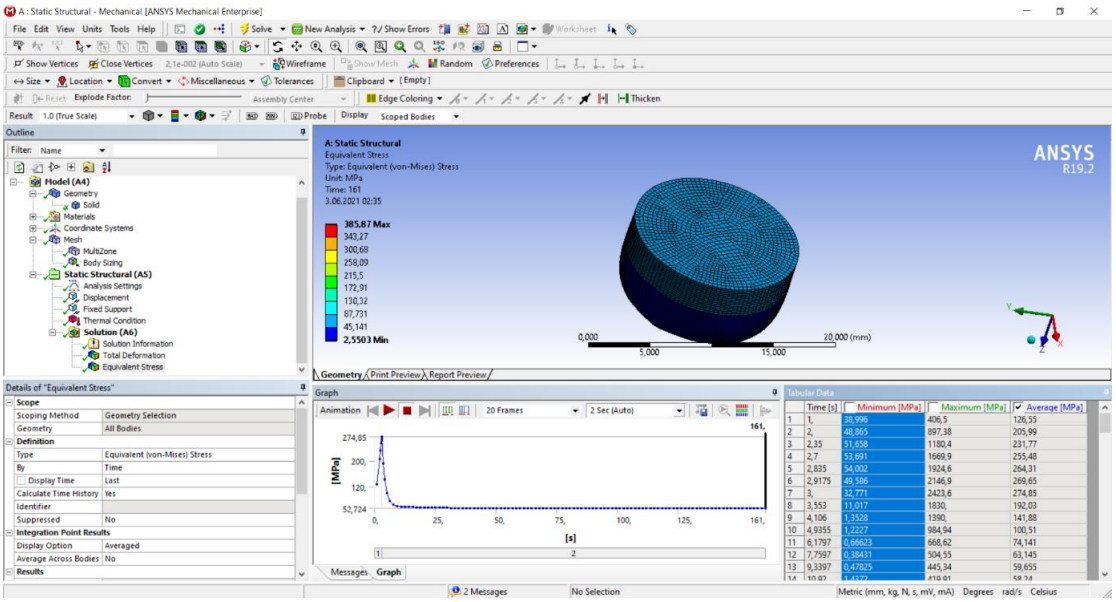

Figure 3.8 The relaxation test results of Araldite LY 564 Epoxy in the ANSYS.

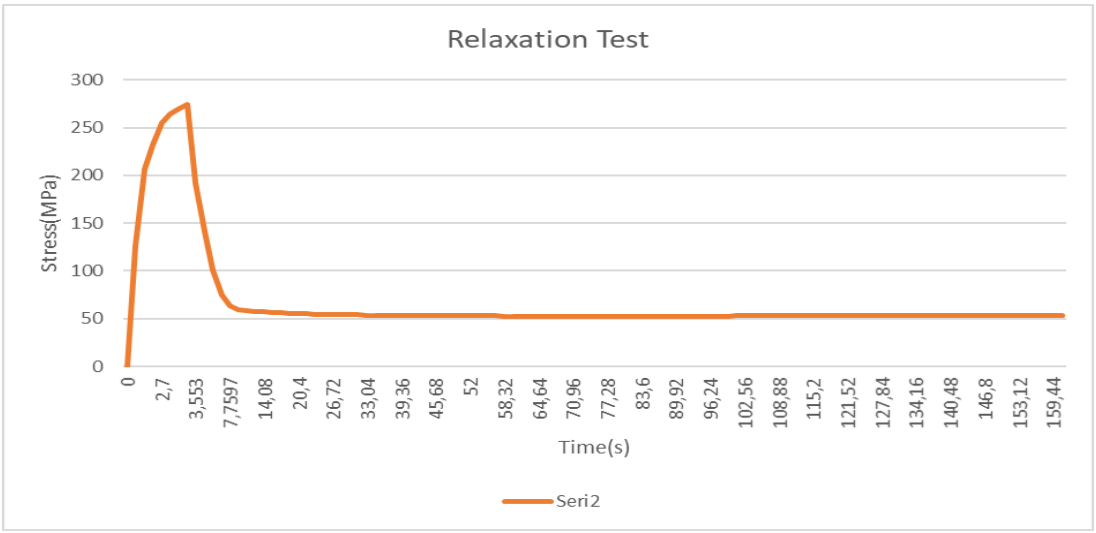

Figure 3.9 The stress-strain graph of the relaxation test according to the ANSYS results.

As can be seen in Fig. 9, the stress-strain graph for relaxation test simulation is obtained in ANSYS. In general perspective, this graph is found to be compatible with the other graphs in literature. For three seconds, the stress value increased and reached its peak just above the 250 MPa. For the rest of the time, the stress relaxation behavior is observed for the viscoelastic material and the stress value dropped to 50 MPa, then stayed constant until the test end.

3.3 ANSYS applications with graphene-epoxy nanocomposite

In this section, graphene-epoxy nanocomposite fabricated in the laboratory, was introduced into the ANSYS. By performing some tests such as airplane wing FSI analysis, electronic card drop analysis, car body crashing analysis, it is aimed that testing the graphene-epoxy for the usage by various sectors to have opinion whether it is applicable or not.

3.3.1 The airplane wing analysis with ANSYS

ANSYS FSI analysis which provides transfer of the Fluid Flow (Fluent) module solutions to the Static Structural module is performed. To apply such analysis, firstly the problem must be solved by using CFD techniques. After solutions obtained in the Fluid Flow (Fluent), there two methods to share the results with the Static Structural module; one is dragging the solutions box of the Fluid Flow (Fluent) module into the setup box of the Static Structural module, the other way is adding system coupling module to combine the Fluent Flow (Fluent) and the Static Structural modules. The first way is preferred in this work.

In this analysis, NACA 0012 airplane wing with a 1-meter chord line and 2-meter length was used as geometry. To perform this analysis, Fluid Flow (Fluent) and Static Structural modules were used, respectively. As the first step of the analysis, the wing geometry was uploaded and prepared for simulation. In the Space Claim section, the angle of attack was defined as 15^{o}, and the enclosure was created. By enclosure feature, a computational domain can be created, and this domain confines the air flows.

After geometry preparation completed, the mesh was created for CFD analysis. Meshing bears crucial importance in terms of obtaining good results and realistic calculations. In the meshing operation, the multizone method was applied because the enclosure multizone method is appropriate for the geometries that have various geometry on each side. Besides the multizone method, sizing methods were used to obtain better mesh quality. Body sizing and sphere of influence methods were inserted on enclosure geometry. Since it is an airflow analysis, the mesh quality around the wing surface is particularly important so, using the sphere of influence method reasonable. In the sphere of influence method, the program creates spheres to points that specified by the

user and by the values that are given, finer and qualified mesh is created by the program. As the last step of the meshing, inflation was given to the body since it is a CFD analysis.

In the setup section of the Fluid Flow (Fluent), the configuration of flow is done by considering it as compressible flow since the velocity value is selected 50 m/s which is a relatively high value. When the flow is considered compressible, the Fluent module of the ANSYS performs calculations according to absolute pressure that is the sum of gauge and operating pressures. To model the compressible flow, operating pressure was taken as zero and the gauge pressure value was calculated with the equation (3.4) and the temperature value calculated with equation (3.5). As a viscous model, the k-omega turbulence model was selected, since the Reynolds number calculated with equation (3.6) is high. By activating the Sutherland principle in viscosity calculation in creating/edit options so, temperature-depending calculating was provided which is appropriate for compressible flow with high velocity. After the boundary conditions were introduced, the solution methods options were arranged as all results will be calculated with high-order equations by activating the coupled theory.

$$\frac{P_0}{P} = [1 + (\frac{\gamma-1}{2}) M^2]^{\frac{\gamma}{\gamma-1}} \quad (3.4)$$

$$\frac{T_0}{T} = 1 + (\frac{\gamma-1}{2}) M^2 \quad (3.5)$$

$$Re = \frac{\rho V L}{\mu} \quad (3.6)$$

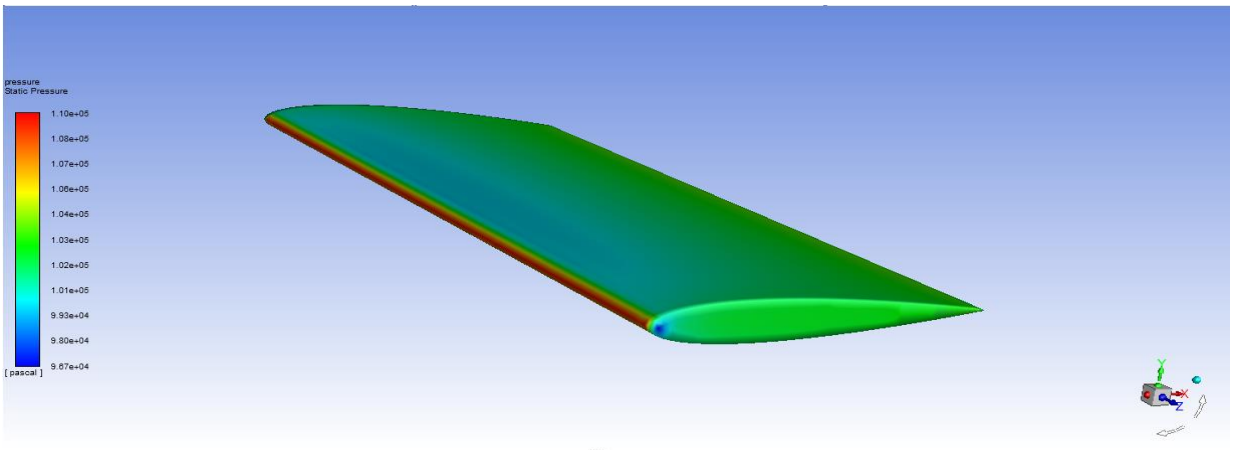

Figure 3.10 CFD analysis results of NACA 0012.

To transfer the CFD results to Static Structural, the solution section of the Fluid Flow (Fluent) module was shared with the setup section of the Static Structural module. The material property definitions of the Graphene Epoxy Nanocomposite were done in

engineering data. Required properties such as density, isotropic elasticity, multilinear isotropic hardening were obtained by the laboratory experiments and introduced to the program. In the model section, the material definition of the body and meshing operation with the body sizing method was done. Since the results of the CFD were sheared with the Static Structural module, by clicking the imported load the pressure values were inserted on the wing-body by the program. The face of the wing bonded with the airplane considered as fixed support.

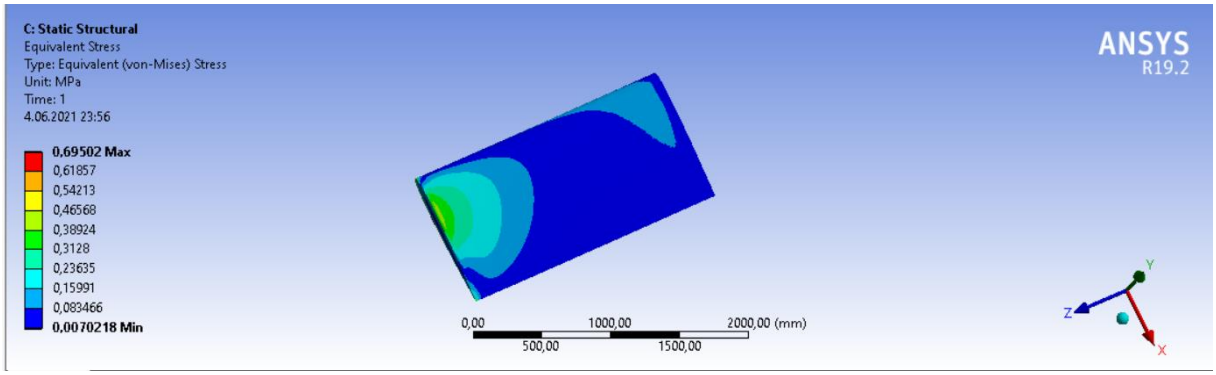

Figure 3.11 The static Structural analysis results of NACA 0012 made from graphene-epoxy (Equivalent Stress).

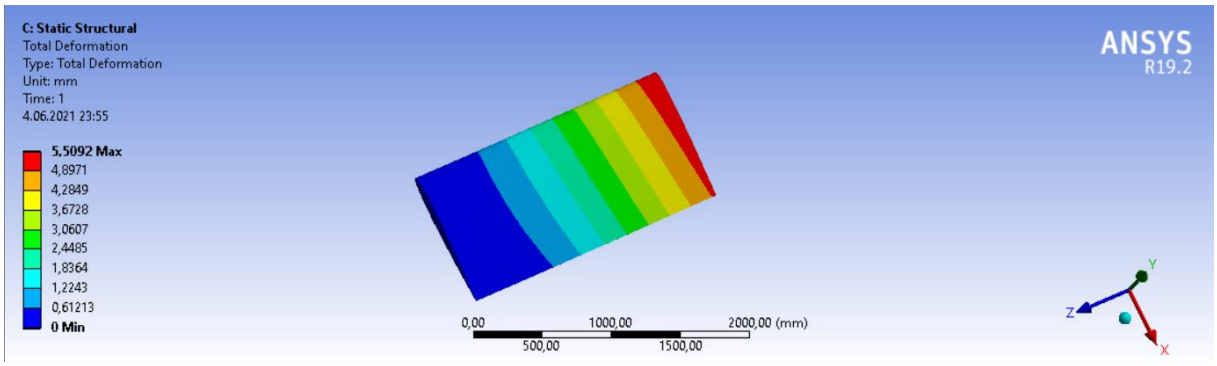

Figure 3.12 The static Structural analysis results of NACA 0012 made from graphene-epoxy (Total Deformation).

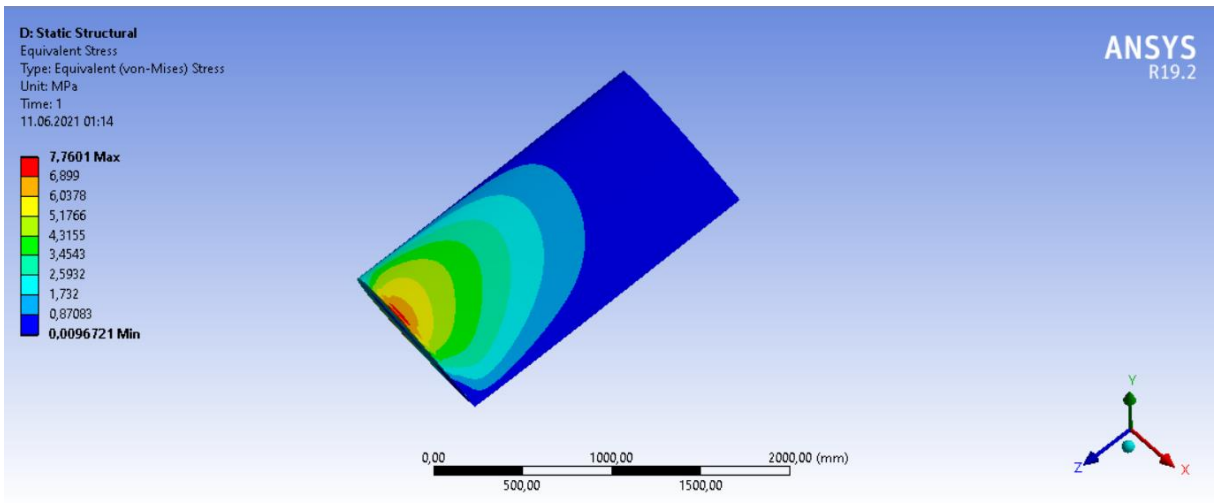

Figure 3.13 The static Structural analysis results of the NACA 0012 made from aluminium alloy (Equivalent Stress).

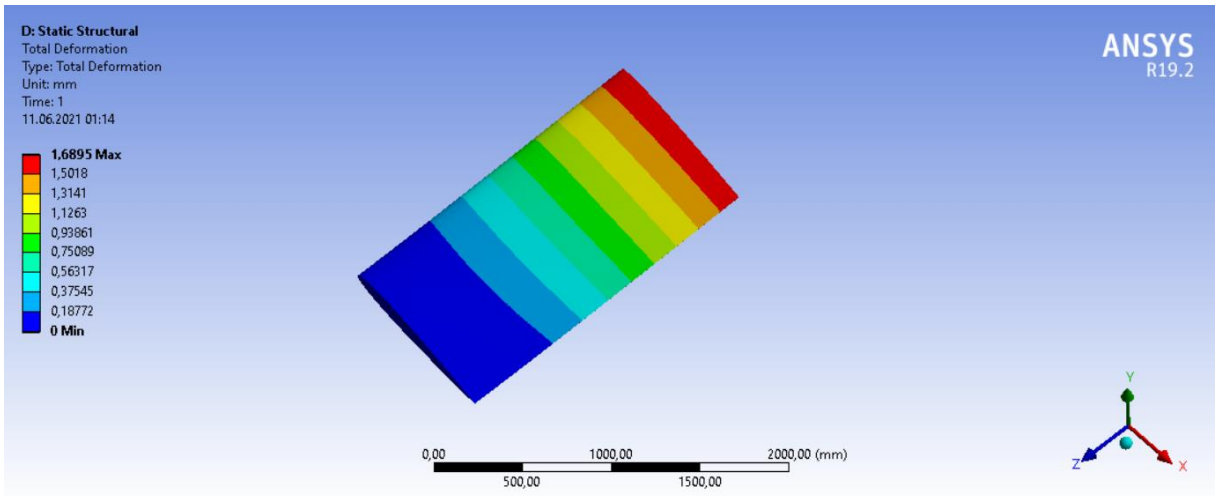

Figure 3.14 The static Structural analysis results of NACA 0012 made from aluminium alloy (Total Deformation).

As it can be seen in figures above, the analysis is performed for graphene-epoxy nanocomposite and aluminium alloy. While the stress values are lesser in the wing made from graphene-epoxy nanocomposite, the total deformation values are lesser in the wing made from aluminium alloy. The stress distributions are similar for each wing, and it densify around the location where wing is bonded with the airplane. The total deformations occurred at the free end of the wings.

3.3.2 The drop test analysis of an electronic card in the ANSYS

The usage area of graphene-based nanocomposite materials is continuing to increase day after day. Besides its mechanical properties, also, thanks to its electrical properties, the popularity of graphene in electronics-related applications is also increasing [9]. The scope of this analysis is to compare the deformations of PCB material generally used for electronic cards and graphene epoxy nanocomposite when the electronic cards made from these two materials are dropped from 1 m height to the ground. To simulate the analysis a rectangular shape with the length of 160 mm, with the height of 93 mm, and with the thickness 2 of mm was used. There are 3 memory cards, a heat sink, and a CPU on the card. The heat sink is made from Al 6063 in both two cards.

To simulate the drop test, the Explicit Dynamic module is used since the drop velocity is relatively high. To conduct such simulations, ANSYS has an extension which name is MechanicalDropTest and it must be activated from the Extensions Manager section before starting to analysis.

PCB, Al6061, graphene epoxy nanocomposite was defined into engineering data by writing density, isotropic elasticity, and plastic behaviour values. In the model section, firstly, the material assignment made for all elements in the geometry. Meshing operation is done by entering element size value and activating capture curvature. In the next step, the drop test wizard feature activated in the environment section. In this extension, drop rotation value defined as -25^{o}, and drop height value defined as 1 m. After editing the drop test wizard extension, the settings automatically arranged by the program. Shell thickness factor arranged as 1 in the body interactions section to let the program assumes the contact surface as physical body imported by the user.

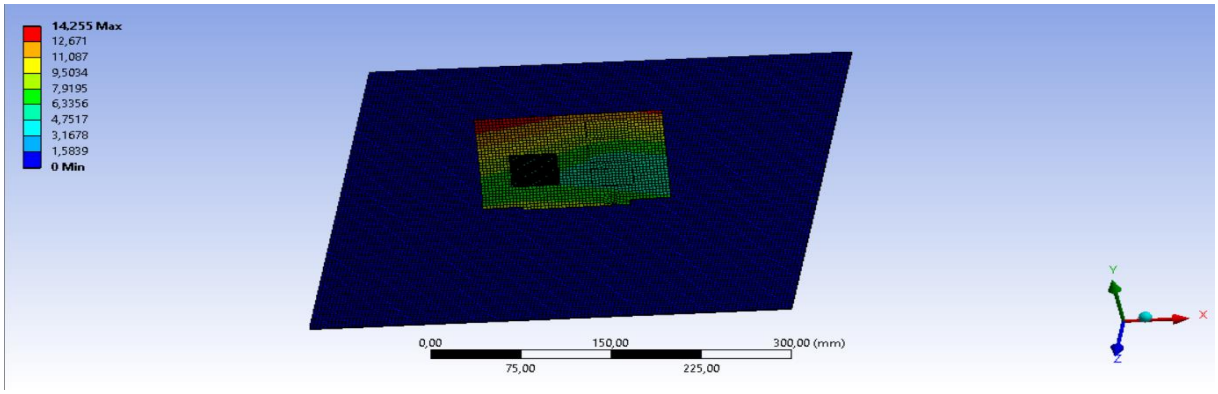

Figure 3.15 The drop test analysis results of the electronic card made from PCB (total

deformation in mm).

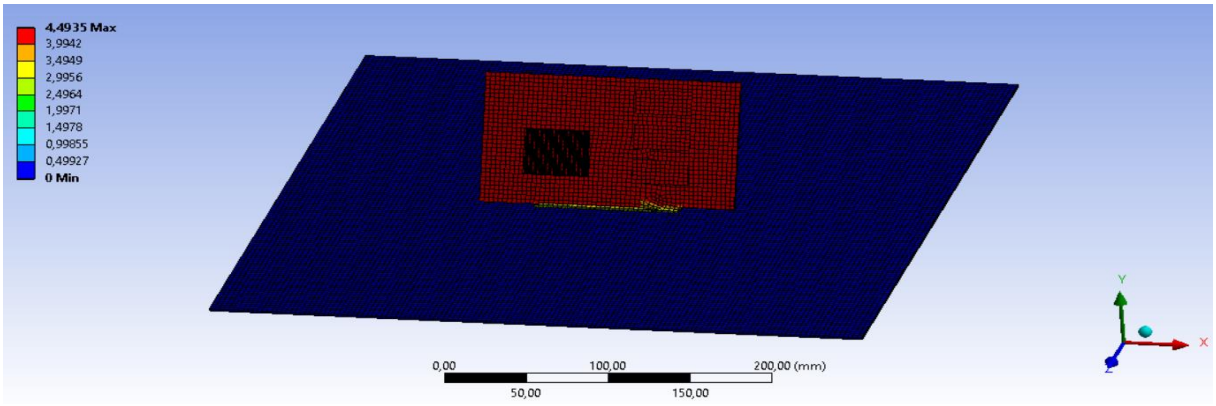

Figure 3.16 The drop test analysis results of the electronic card made from graphene epoxy (total deformation in mm).

3.3.3 The car body crashing test analysis in the ANSYS

The studies of the usage of graphene-based nanocomposite materials in the automotive sector already started and the various beneficial aspects of graphene's superior features applied to the cars in miscellaneous ways. In this work, an analysis performed for a car body with nearly the same dimensions as real ones. For this analysis, the Explicit Dynamics module used since the velocity value of the car body is remarkably high.

To define material to the program, density, isotropic elasticity, multilinear isotropic hardening properties were written in the engineering data section. The point that should be noticed for the defining multilinear isotropic hardening is only 10 pieces of stress-strain data can be used in the Explicit Dynamics modulus. After that, the car body imported to the geometry section, the geometry has approximately 4,4 m length and 1,7 m width. The thickness value assumed as 1,2 mm since such analysis with realistic dimensions can take a long time and cannot be solved by computers with low capacity so, working small thickness value helps to get results in a shorter time.

In the model section, mesh operation done with the body sizing method. To prevent occurring intersect surfaces between the car body and barrier, offset type arranged as a top for barrier and bottom for the car body. All edges of the barrier introduced as fixed support to the program. The displacement value was given as 0 in the z-axis to the

program and implemented to all bottom edges of the car body. 0,0009s end time was defined as the analysis setting since the CPU capacity is not enough for analysis that takes a longer time. Since the analysis was performed for a small-time value, 360 km/h a high-velocity value was given to the car body in the scope of getting more realistic results.

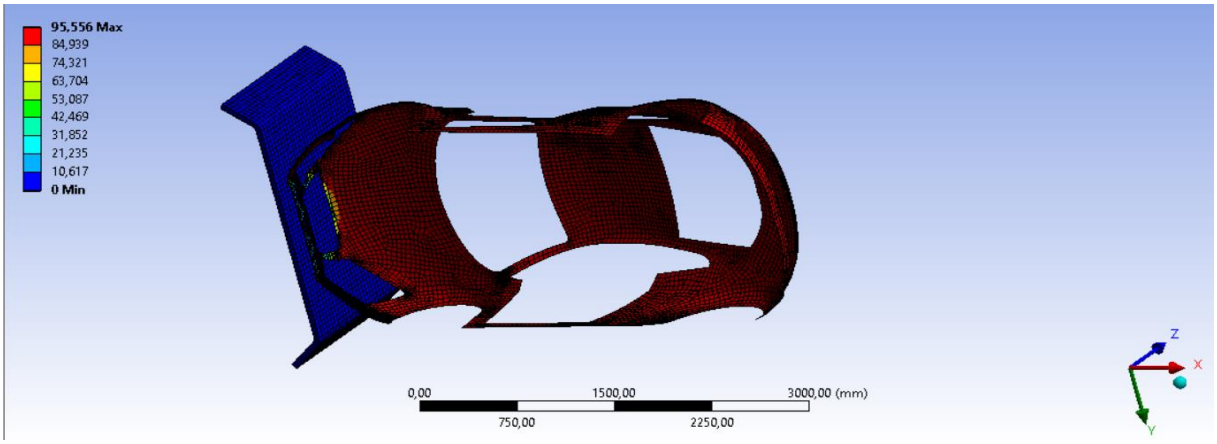

Figure 3.17 The car body made from graphene-epoxy nanocomposite crash analysis result (total deformation in mm).

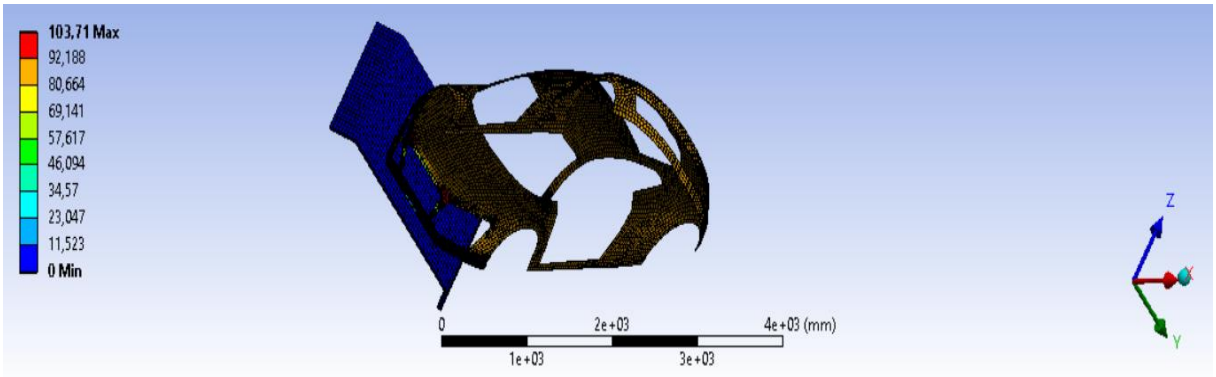

Figure 3.18 The car body made from aluminum alloy crash analysis result (total deformation in mm).

As it can be seen in the figures above, in the results of the crash simulations, the car body made from aluminum alloy deformed more than the car body made from graphene-epoxy nanocomposite. For the car body made from aluminum alloy, yellow contours can be seen in most of the points of the car body which means deformation for this body is around 90 mm. So, it can be deduced that deformation amounts for two-car bodies made from different materials nearly the same for the same time periods.

4. ENVIRONMENTAL IMPACT ASSESMENT AND SUSTAINABILITY

The environmental and health impacts of graphene-based nanomaterials is a controversial issue that must be investigated detailed. Although no information on graphene emissions at work was discovered in the literature, several researchers contacted expressed concern that workplace or laboratory emissions may lead to cutaneous or pulmonary exposure. Based on chemical principles, graphene does not appear to be volatile due to its huge size. Graphene is not volatile, according to the majority of academics polled. However, according to the researchers questioned, graphene may bond to airborne particles such as dust particles, resulting in lung exposure [10].

5. CONCLUSION

In this thesis, viscoelastic behavior and modeling viscoelasticity in numerical analysis programs were investigated. Also, fabrication of the graphene-epoxy nanocomposite material which was produced in Yıldız Technical University Central Laboratory was presented. Some ANSYS applications that used graphene-epoxy nanocomposite were performed and results compared with applications that used other materials. As result, Using the Prony Series method is available for finite element programs to define viscoelastic behaviors of the materials. To apply this method, the only requirement is obtaining experimental data, and numerical analysis programs can calculate Prony Series values appropriately. While modeling an experimental test such as relaxation, compression e.g., the critical point is time configuration. Since it takes a long time to perform such tests, modeling these tests in a numerical program requires a computer with a qualified CPU. Another critical factor is the time step, both quasi-static compression test and relaxation test should be conducted with small step sizes which leads to total time is extended. As for the ANSYS application with graphene-epoxy nanocomposite material, the results of these applications compared with the applications used other popular material and shows that graphene-epoxy nanocomposite is an applicable material for the various sector. For the NACA 0012 application, when comparing, while the maximum total deformation of the wing made from graphene-epoxy is 4 times larger than the wing made from aluminum alloy, the total stress value of the wing made from aluminum alloy is 10 times larger than the wing made from graphene-epoxy. It must be noticed that the density of the aluminum alloy is 7 times larger than the density of the graphene-epoxy. When it comes to the electronic card drop test, the electronic card made from PCB which is a popular material for this sector deformed more than graphene-epoxy. Lastly, in the car body crash application, the total deformation amount is close to each other for aluminum alloy and graphene-epoxy. These applications can give general information. It is known that graphene is a new material that increasingly popular and needs to be developed. It can be said that with the superior features of graphene, the nanocomposites of this novel material can be adapted to various sectors easily. There are many mysterious about graphene in terms of environmental and health issues that must be investigated. Since, serial production of graphene-based nanocomposite is hard and requires high cost, in the future, it is predicted that graphene-based nanocomposite will be prevalent using material in different sectors.

6. REFERENCES

[1] Callister, W. D., & Rethwisch, D. G. (2009). Material Science And Engineering: An Introduction (8th Edition). USA: John Wiley & Sons.

[2] Shaw, M. T., & MacKnight, W. J. (2018). Introduction The Polymer Viscoelasticity (4th Edition). New Jersey: John Wiley & Sons.

[3] Ferry, J. D. (1980). *Viscoelastic Properties Of Polymers(3th Edition).* Wisconsin: John Wiley & Sons.

[4] Wei J., Vo T., Inam F. '' Epoxy/graphene nanocomposites – processing and properties: a review.'' RSC Adv**.**, 2015,**5**, 73510-73524. https://doi.org/10.1039/C5RA13897C

[5] Çolak, Ö., Bakbak, O., Birkan, B. E., & Acar, A. (2021). Mechanical characterization of Araldite LY 564 epoxy. Polymer Bulletin, 1, 17. https://doi.org/10.1007/s00289-021-03624-x

[6] Colak, Özgen U., Bahlouli N., Uzunsoy D., Francart C. "High Strain Rate Behavior of Graphene-Epoxy Nanocomposites." Polymer Testing, vol. 81, 2020, p. 106219., doi:10.1016/j.polymertesting.2019.106219.

[7] Fettahoğlu, A. ''Effect of time step size on stress relaxation''. CJSMEC, 2016. https://doi.org/10.20528/cjsmec.2016.11.029

[8] Zheng Z., Zhang R. ''Implementation of a Viscoelastic Material Model to Simulate Relaxation in Glass Transition.'' Corning Incorporated, Corning, NY, USA, 2014.

[9] Ganesh Ram, R.K., Cooper, Y.N., Bhatia, V., Karthikeyan, R., Periasamy, C., 2014. Design Optimization and Analysis of NACA 0012 Airfoil Using Computational Fluid Dynamics and Genetic Algorithm. AMM 664, 111–116. https://doi.org/10.4028/www.scientific.net/amm.664.111

[10] Jiajie Liang, Yongsheng Chen, Yanfei Xu, Zhibo Liu, Long Zhang, Xin Zhao, Xiaoliang Zhang, Jianguo Tian, Yi Huang, Yanfeng Ma, and Feifei Li

ACS Applied Materials & Interfaces 2010 2 (11), 3310-3317

DOI: 10.1021/am1007326

[11] Fadeel B., Busy C., Merino S., Vázquez E., Flahaut E., Mouchet F., Evariste L., Gauthier L., Koivisto A. J., Vogel U., Martín C., Delogu G., Buerki-Thurnherr T., Wick P., Beloin-Saint-Pierre D., Hischier R., Pelin M, Carniel C., Tretiach M., Cesca F., Benfenati F., Scaini D., Ballerini L., Kostarelos K., Prato M.
ACS Nano 2018 12 (11), 10582-10620
DOI: 10.1021/acsnano.8b04758

[12] Dunn, L. ''Introduction to Viscoelasticity in Polymers and its Impact on Rolling''. International Journal of Squiggly and Wobbly Materials, v23, 1, 2019.

[13] Chen, T. ''Determining Prony Series For A Viscoelastic Material From Time Varying Strain Data.'' NASA Langley Technical Report Server, 2000.

[14] Zienkiewicz, O. C., Taylor, R. L., & Zhu , J. Z. (2005). The Finite Element Method: Its Basis and Fundamentals (6th Edition). Oxford: Butterworth&Heinemann.

[15] Kalidindi, S. R., Abusafieh, A., & El-Danaf, E. ''Accurate characterization of machine compliance for simple compression testing''. *Experimental Mechanics* , 210-215, 1997.

[16] Shrivastava, A. ''Plastic Properties and Testing . Introduction to Plastics Engineering'' , 49-110, 2018.

[17] Cerrada , M. L. (2005). Introduction to the Viscoelastic Response in Polymers, 167-182 . ISBN: 84-9749-100-9